NASA Technical Memorandum 79124

WIND TUNNEL PERFORMANCE OF FOUR ENERGY EFFICIENT PROPELLERS DESIGNED FOR MACH 0 8 CRUISE

by Robert J Jeracki Daniel C Mikkelson,
and Bernard J Blaha
Lewis Research Center
Cleveland, Ohio

TECHNICAL PAPER to be presented at the
Business Aircraft Meeting
sponsored by the Society of Automotive Engineers
Wichita, Kansas, April 3-6, 1979

THE INCREASED EMPHASIS on fuel conservation has stimulated a renewed interest in turboprop powered aircraft. Studies by NASA and industry on aircraft designed for Mach 0.8 cruise above 9.144 km (30 000 ft) altitude indicate significant block fuel savings and direct operating cost reductions of turboprop powered aircraft over comparable turbofan powered aircraft. Specific studies and summaries are given in Refs. (1)* to (34). A recent status report on NASA's Advanced Turboprop Project, which is part of its Aircraft Energy Efficiency Program, is discussed in Ref. (2). High speed turboprop propulsion has been studied for a variety of subsonic aircraft applications, both civil and military. The magnitude of the fuel savings of turboprop powered aircraft over comparable technology turbofan powered aircraft is generally influenced by aircraft cruise speed and operating range. This is shown in the trend curves of block fuel savings versus operating range shown in Fig. 1 from Ref. (2). Fuel savings from 15 to 30% at Mach 0.8 may be realized by the use of an advanced high-speed turboprop. The Mach 0.7 cruise aircraft show larger fuel savings than those designed for Mach 0.8 since the advantage of the high speed turboprop propulsion system over the turbofan increases as Mach number is decreased. Fuel savings of over 20% may be realized at Mach 0.7 for ranges typical of business jet aircraft. The fuel savings also increases for shorter stage length operation because a larger portion of the block time is spent at the lower speeds of climb and descent where turboprop propulsion offers even larger advantages. These projected aircraft fuel savings with the high speed turboprop have a significant impact on the aircraft direct operating cost. Since fuel costs about 40% of the direct operating cost (DOC) of medium-to-short haul commercial aircraft, a 20 to 25% fuel savings results in an 8 to 10% lower DOC (2). Fuel savings are greater (22) for longer range aircraft and so the DOC savings are greater. Very long range aircraft can take advantage of reduced fuel consumption to reduce aircraft weight and size which gives additional DOC reduction as well as reducing acquisition cost and lower life cycle cost. The variation of DOC savings with fuel costs from Ref. (16) is shown in Fig. 2. The curves are based on earlier studies with both 1985 technology assumptions and also 1976 technology (16,23-24). Boeing and Lockheed examined 1985 technology level turboprop engines versus equivalent technology level turbofan engines. The Boeing aircraft design was based on 1976 technology levels while Lockheed used 1985 technology levels. Douglas used the DC9-30 as a basis of comparison and compared both current technology turboprop engines and 1985 technology level engines to the current DC9-30 configuration using low-bypass-ratio JT8D turbofan engines. As can be seen, a wide spread in DOC savings was achieved, reflecting the various assumptions of propeller efficiency, fuselage design and weight for noise attenuation, aircraft configurations, design stage lengths, maintenance costs, etc. In all cases, however, there is a very significant improvement for the turboprop powered aircraft. This is especially true at the shorter stage lengths making advanced turboprops look particularly attractive for the short-and-medium-range markets.

ADVANCED DESIGN CONCEPTS

Most of the aircraft studies have been based on estimated propulsive efficiency from the propeller near 79.5% at Mach 0.8. To achieve this level of performance with an acceptable cabin noise level, several advanced aerodynamic and acoustic concepts were evaluated and used in designing the present wind tunnel models. These concepts have been discussed in previous reports (1,2,35-37) and will mainly be summarized here. Figure 3 schematically describes these important design concepts for high speed propeller design. They include reduced blade thickness and tip sweep to minimize compressibility losses in the outboard part of the blades and to reduce cruise noise; tailored nacelle blockage and spinner area-ruling to reduce blade-to-blade choking and other compressibility losses in the blade root region; and, the use of advanced airfoil technology. To hold propeller diameter and weight to reasonable values for Mach 0.8 cruise above 9.144 km (30 000 ft) altitude, power (disk) loadings several times higher than conventional design are required. These high loadings then would require increasing the number of blades to around 8 to 10 to keep ideal propeller efficiency high. Advanced propeller/nacelle design is a highly integrated procedure and is

*Numbers in parentheses designate References at end of paper.

described in detail in Ref. (1). An example of this integrated procedure is shown in Fig. 4 where blade sweep, spinner area ruling and nacelle blockage are used to minimize compressibility losses across the complete blade radius. For a straight propeller at the design condition of Mach 0.8 cruise and 243.8 m/sec (800 ft/sec) blade tip speed, all section relative Mach numbers (curve A) are above the drag divergence Mach number (curve B) of the propeller with NACA 16-series airfoils even when thin blade sections are used. Adding 30° of sweep (curve C) brings the Mach numbers near the tip to values lower than drag divergence levels. Area-ruling the spinner and nacelle blockage suppress the local Mach numbers in the hub region (curve D). All of the advanced aerodynamic and acoustic concepts were investigated in the wind tunnel model program discussed here with the exception of advanced airfoils. Under current NASA plans, this concept will be addressed in the future.

In addition to the propulsive efficiency goals, near-field source noise target levels were established to keep interior noise levels competitive with current wide body aircraft and to minimize the need for fuselage treatment. Since the blade relative tip Mach numbers are slightly supersonic as shown in Fig. 4 ($M_{TIP} \approx 1.14$) the initial approach for noise reduction was to add sweep and reduce the effective local section Mach number to below the section critical Mach number. The shock strength and therefore the resulting pressure pulse is thereby reduced. The 30° tip sweep blade designs were expected to be somewhat quieter for this reason. A more advanced concept was incorporated in a 45° tip sweep design (SR-3) using the linear acoustic analysis of Ref. (38). A historical development of the application of acoustic theory to advanced propeller design is given in Ref. (39). The present theory predicts thickness (due to blade airfoil thickness distribution) and loading (due to pressure loads on the blade airfoil) noise components from each radial section of the blade. Thickness noise is generally the dominant noise source on a propeller operating with a slightly supersonic tip Mach number. By properly sweeping the blade plan form it is possible to reduce near-field noise using the phase interference concept illustrated in Fig. 5. The noise from one propeller blade is the vector sum of the contributions of the sinusoidal wave (amplitude and phase angle) from each radial strip. The noise of the total propeller is the product of the vector sum and the number of blades. Sweeping the tip back causes its signal to lag (increased phase angle) the signal from the mid blade region thus causing partial interference and a reduction in noise. This phase interference concept was used in the acoustic design of the 45° swept propeller model (SR-3) to reduce the near-field cruise noise. This concept should have application to both thickness and loading noise in the near and far fields.

MODEL DESIGN AND TESTS

Initial design studies (36) for high speed propellers were based on comparisons with present day turbofan powered transports, with the requirement that airplane speed, cabin environment, and airplane safety not be degraded with an advanced fuel efficient turboprop. The design Mach number of 0.8 and altitude over 9.144 km (30 000 ft) was established to allow turboprop powered aircraft to mesh with turbofan powered aircraft. High propeller power (disk) loading is required without the size and weight penalty associated with conventional propeller designs to achieve the Mach 0.8, 10.668 km (35 000 ft) design point. All the advanced propeller designs that were tested had eight blades with blade activity factors near 200 (except 235 for SR-3) to meet this high loading requirement. In order to keep the airplane cabin noise comparable to present turbofan powered aircraft, an aerodynamic - acoustic compromise was reached in the initial propeller designs which allowed the relative tip Mach number to be slightly supersonic (approx. Mach 1.14). The design parameters for the four model propellers that were tested are shown in Fig. 6 along with the predicted design point efficiencies from the method of Ref. (1). Also, the predicted cruise noise using the acoustic analysis of Ref. (39) at flight conditions and a distance of 0.5 propeller diameters from the tip is shown.

As can be seen, tip speed, power loading, and blade number for all four designs were the same, therefore ideal efficiency was the same for all of the designs. All designs had thin airfoils with wide chords and had twist and

camber distributions which were based on the propeller operating in the flow field around a specific spinner and nacelle. Configuration SR-2 was a straight blade which was designed and tested with an area-ruled spinner (AR-2). SR-1 had 30° of tip sweep and was designed and tested with a conic spinner (C-1). SR-1m was a modification of the SR-1 design with higher loading near the tip. As shown in Fig. 7, this was accomplished by reducing the twist and increasing the camber near the tip compared to SR-1. SR-1m was tested with both the conical and area-ruled spinners. SR-3 had 45° of tip sweep and was the most advanced design so far. The acoustic phase interference concept discussed earlier was used in the design of the plan form shape (chord and sweep). SR-3 was predicted to have a noise level about 6 dB below the straight bladed SR-2 design. SR-3 was designed and tested with an area-ruled spinner (AR-3). As shown in Fig. 6, the predicted design point efficiency increased as the amount of sweep was increased. The blade geometry characteristics for all four blade designs are shown in Fig. 7. Airfoil sections for the blade designs were NACA series-16 from the tip to the 53% radius (45% for SR-1) and NACA series 65 with circular arc mean line (NACA a = 1 mean line for SR-1) from the 37% radius to the root with a transition fairing between.

At their design advance ratio (J = 3.06) and power coefficient (Cp = 1.7) the predicted efficiencies are presented in Fig. 8 at free-stream Mach numbers from 0.6 to 0.85. For reference the ideal efficiency level (85.1%) is shown which was based on an optimum blade loading with zero blade drag. The predicted efficiencies were all high at low Mach numbers with the 45° sweep SR-3 propeller and the 30° sweep SR-1m propeller just about 1% above the 30° sweep SR-1 and 0° sweep SR-2 propellers. Significant differences associated with sweep appeared above Mach 0.7. The 30° swept configurations showed about a 2% improvement compared to the straight SR-2 propeller. The 45° sweep SR-3 propeller showed even higher performance and the predicted efficiency remained above 80% out to Mach 0.85.

The 62.2 cm (24.5 in.) diameter propeller models were all tested in the NASA Lewis 8-by-6 foot wind tunnel (40) on the 1000 hp propeller test rig (PTR). Figure 9 shows the 45° swept SR-3 model installed on the PTR. A cutaway drawing of the PTR is shown in Fig. 10. The propeller models were driven by a three stage air turbine using a 3.103×10^{6} N/m^2 (450 psi) continuous flow air supply system. Forces on the propeller and spinners were measured using two separate systems. A load cell located in the vertical strut was used to measure axial force. A rotating balance located just aft of the spinner measured both thrust and torque. Nacelle forces were determined from pressure integration.

The wind tunnel tests were conducted at zero model incidence to the free-stream flow. The blade angle measured at 3/4 propeller radius ($\beta_{3/4}$) was set at various angles and data were taken over a range in Mach number from 0.6 to 0.85.

AERODYNAMIC TEST RESULTS

The wind tunnel performance data in this paper are presented in terms of propeller net efficiency. That is, the propulsive efficiency of the propeller blades alone, after correcting for isolated spinner drag and the buoyancy interaction force from the nearby nacelle. The buoyancy correction force was determined using the method of Refs. (41) to (43). Net efficiency (η_{NET}) and power coefficient (Cp) plots at Mach 0.6 and 0.8 are presented in Fig. 11 for SR-3. The coefficients were based on a reference propeller diameter of 62.2 cm (24.5 in.) which was the actual diameter with the blades in the approximate feather position. For the swept models the diameter at cruise blade angles was slightly larger than this. The propeller diameter changes with blade angle setting due to the blade sweep.

At each blade angle and Mach number the propellers were operated at a number of power levels to obtain the variation of net efficiency and power coefficient with advance ratio shown in Fig. 11. Power loading (SHP/D^2) can be written in terms of propeller coefficients and free-stream conditions as:

$$\frac{SHP}{D^2} \propto \frac{P}{D^2} \equiv \frac{Cp}{J^3}\left(\rho_o V_o^3\right)$$

From this relationship lines of constant power loading have been added to Fig. 11 as percentages of design loading parameter Cp/J^3 (= 0.05933) determined at the design operating

conditions of J = 3.06 and Cp = 1.7. Performance at constant power loading were plotted from these basic data curves. The effect of power loading and advance ratio on net efficiency at Mach 0.6 and 0.8 is shown in Figs. 12 and 13, respectively. Each propeller/spinner combination that was tested is presented as a separate plot. Typical variation of efficiency with advance ratio at a constant power loading is a peaked curve. The reduction from the peak with increasing advance ratio is due to a combination of lower ideal efficiencies due to increased swirl and lower blade sectional lift to drag ratios (from increasing local angles of attack). The fall-off with decreasing advance ratio is due to increased compressibility losses associated with the higher tip rotational speeds and/or again lower blade sectional lift to drag ratios (from decreasing local angles of attack).

At Mach 0.8 the performance drop at low advance ratios appeared more severe for the straight SR-2 model than for the swept configurations most likely indicating earlier onset of compressibility losses in the blade tip region. At both Mach 0.6 and 0.8 SR-1m appeared to have less performance loss at the high advance ratios than SR-1 which may be due to a more optimum twist and camber distribution. Addition of the area-ruled spinner to the SR-1m model improved the performance at Mach 0.8 from low to high advance ratios indicating a possible reduction in losses in the blade root region. The 45° swept model (SR-3) which had an area-ruled spinner appeared to get most of its performance benefit at low advance ratios, when compared to the best 30° swept model (SR-1m) with the area-ruled spinner. This indicates benefit from the increased sweep in reducing onset of compressibility losses at the blade tips.

In general the effect of reduced power loading was an improvement in performance. However, the aircraft tradeoff that occurs is increased propeller size which can affect the overall airplane design and may cause increased weight and cost penalties. The increased performance may more than make up for this penalty, but this will depend on the specific application. A thorough airplane mission analysis study can determine the desirability of modifying the propeller "design point" to optimize the overall performance.

Performance at the 100% power loading and design advance ratio of 3.06 were obtained from the crossplots in Figs. 12 and 13, and also at other Mach numbers from similar crossplots. A design loading performance summary of measured net efficiency over the Mach number range from 0.6 to 0.85 is presented in Fig. 14. Comparing the configurations at Mach 0.8 indicates that each step in design improvement did yield an improvement in efficiency that approached the study values used in fuel efficiency comparisons between turboprop and turbofan powered aircraft. The 30° sweep of SR-1 and SR-1m yielded about 1% improvement (77%) over the straight SR-2 blade efficiency of 75.8%. Adding the area-ruled spinner to SR-1m improved its performance about an additional percent to near 78%. The SR-3 model with its 45° of sweep and area-ruled spinner had the highest performance (78.7%) at the design Mach number of 0.8 and had significant benefit out to Mach 0.85. The improvement over the SR-2 (0° sweep) configuration was about 3% at design. At Mach 0.6 and 0.7 the SR-1m (30° sweep) and SR-3 (45° sweep) configurations had nearly the same efficiency of about 81%. These results are quite encouraging and future models with 10 blades and lower power loading should have even higher performance.

ACOUSTIC TEST RESULTS

In addition to the performance data, acoustic measurements were also made in the Lewis 8-by-6-foot wind tunnel on the following models: SR-2 (0° sweep), SR-1m (30° sweep) with the conical spinner, and SR-3 (45° sweep). These data were obtained from six wall-and-ceiling-mounted pressure transducers as shown in Fig. 15. Measurements were made with the propellers operating at near-design condition over the Mach number range from 0.6 to 0.85, and also at feather conditions for the SR-3 model. Though the porous-walled tunnel does not have acoustic damping material on any of its walls and absolute noise levels may be subject to question because of reflections, the data obtained indicated that information about the noise differences among the three propellers was usable.

Narrow band analysis from 0 to 10 000 Hz, with a bandwidth of approximately 26 Hz, are

presented in Fig. 16 comparing SR-3 (45° sweep) at cruise and feather conditions for a ceiling-mounted transducer slightly downstream of the propeller plane. The propeller blade passage tone and harmonics are visible above the background level (blade at feather) indicating that tunnel background noise was not a problem in comparing relative tone levels. Though it is not possible to prove conclusively that the tunnel noise data are free of reflection caused errors, there are indications that the problem was not severe. There was significant directivity indicated by the ceiling pressures further documented in Ref. (44). Data from the sidewall transducers also indicated a reduction in noise level with distance. Directivity and noise falloff with distance indicate that the tunnel reflections do not everywhere dominate direct incident noise signals. It may be that the tunnel bleed holes and high tunnel velocity did not allow the buildup of a high reverberant level. These observations indicate that at least relative tone level comparisons between blade designs are good.

A comparison of measured noise reduction referenced to SR-2 (0° sweep) is given in Fig. 17 from transducer position 3. SR-1m (30° sweep) is seen to have been slightly quieter than SR-2. The aerodynamic sweep of SR-1m was expected to reduce the noise level somewhat due to lower strength shock waves on the 30° swept blade tip. SR-3 (45° sweep) was about 5 to 6 dB quieter than SR-2 at the blade passage tone. This significant noise reduction was in good agreement with the predicted value from the acoustic analysis program (Fig. 6), where a phase interference concept was used to acoustically design SR-3.

FUTURE PLANS

The advanced turboprop project has been focused on the technology needs of future advanced commercial aircraft. However, the encouraging propeller performance and noise results presented in this paper should have application to business aircraft especially those in the higher performance categories. Future NASA plans for this project include testing of four additional propeller models that will evaluate the following advanced features: increased blade number, aeroacoustic airfoils, lower power loading and alternate design conditions, and increased sweep. Several advanced propeller aerodynamic and acoustic analysis programs have recently been developed or are under development that should enhance the design of these new models. These programs include: an integrated propeller/nacelle analysis for single and dual rotation propellers, a three dimensional transonic lifting surface analysis, and a frequency domain acoustic analysis with nonlinear quadrupole noise sources (39). In addition to the planned work in aerodynamics and acoustics, the Advanced Turboprop Project will address advanced technology in propeller aeroelastics, blade structures and fabrication techniques. The advanced propeller technology work under this project can be extended to lower speed general aviation aircraft. Work presently underway at NASA and included in plans for a program called GAP, for General Aviation Propeller technology, treats performance, noise, aeroelastics, and composite structures in this lower speed range.

CONCLUDING REMARKS

For the advanced turboprop to be competitive with proposed advanced turbofan powered aircraft, it must have high propulsive efficiency at Mach 0.8 cruise above 9.144 km (30 000 ft) altitude with an acceptable cabin noise environment. This goal requires the incorporation of several advanced aerodynamic and acoustic concepts. The propeller needs to be designed integrally with the local nacelle flow field and take advantage of all the aerodynamic suppression possible to overcome the inherent compressibility losses at these high cruise speeds. Four 8-bladed propeller models were designed employing various concepts to reduce compressibility losses. Results from the wind tunnel tests were encouraging. Each design concept appeared to give some performance benefit. The aeroacoustically designed configuration (SR-3) with 45° of tip sweep and an area-ruled spinner yielded the highest propulsive efficiency (78.7% at Mach 0.8, 3.06 advance ratio, and 1.7 power coefficient), with an improvement of approximately 3% over the straight bladed configuration (SR-2). The phase-interference, concept for noise reduction used in SR-3

yielded about 5 to 6 dB reduction compared to SR-2. Advanced aerodynamic and acoustic design techniques have improved propeller performance significantly for high speed applications. Continued refinement including advanced airfoils, increased sweep, larger blade number, and lower tip speeds and power loadings can be expected to make further progress in this important area of more energy-efficient propulsion systems.

SYMBOLS

A	noise amplitude
AF	blade activity factor = $\frac{100\ 000}{16} \int_{\text{hub}}^{r/R=1.0} b/D(r/R)^3 d(r/R)$
AR	aspect ratio
b	elemental blade chord, cm (in.)
Cp	power coefficient = $P/\rho_o n^3 D_{REF}^5$
C_{LD}	elemental blade design lift coefficient
C_{Li}	integrated design lift coefficient $= \int_{\text{hub}}^{r/R=1.0} C_{LD}(r/R)^3 d(r/R)$
C_T	thrust coefficient = $T/\rho_o n^2 D_{REF}^4$
D	blade tip diameter, cm (in.)
DOC	direct operating cost
D_{REF}	reference blade tip diameter = 62.2 cm (24.5/12 ft)
dB	decibel
dCp/d(r/R)	elemental power coefficient $\left[Cp = \int [dCp/d(r/R)]\, d(r/R)\right]$
$dC_T/d(r/R)$	elemental thrust coefficient $\left[C_T = \int [(dC_T/d(r/R)]\, d(r/R)\right]$
J	advance ratio, V_o/nD_{REF}
LH	horizontal distance from PTR centerline, cm (in.)
LV	vertical distance from PTR centerline, cm (in.)
M	Mach number
M_ℓ	local Mach number
M_o	free-stream Mach number
n	rotational speed, revolutions per second
P	power, kW (ft-lb/sec)
PTR	propeller test rig
R	blade tip radius, cm (in.)
r	radius, cm (in.)
SHP	shaft power, kW (hp)
SR	single rotation
T	thrust, newtons (lb)
t	elemental blade thickness, cm (in.)
V	local velocity, m/sec (ft/sec)
V_o	free-stream velocity, m/sec (ft/sec)
V_{TIP}	blade rotational tip velocity, m/sec (ft/sec)
Z	axial distance from propeller plane of rotation, cm (in.)
β 3/4	blade angle at 75% radius, deg
$\Delta\beta$	effective blade twist, deg

η_{APP}	apparent efficiency = $(T_{APP} \cdot V_o)/P$
η_i	ideal propulsive efficiency = $(T_{ideal} \cdot V_o)/P$ (excludes blade profile drag and compressibility losses)
η_{net}	net efficiency = $(T_{net} \cdot V_o)/P$
θ	nominal angle of pressure transducer position from propeller, deg
ρ_o	free-stream density, kg/m^3 ($slugs/ft^3$)
ϕ	phase angle

REFERENCES

1. D. C. Mikkelson, et al., "Design and Performance of Energy Efficient Propellers for Mach 0.8 Cruise." NASA TM X-73612, 1977.

2. J. F. Dugan, Jr., B. S. Gatzen, and W. M. Adamson, "Prop-Fan Propulsion - Its Status and Potential." SAE Paper 780995, SAE Aerospace Meeting, San Diego, Nov. 1978.

3. G. A. Kraft and W. C. Strack, "Preliminary Study of Advanced Turboprops for Low Energy Consumption." NASA TM X-71740, May 1975.

4. "Energy Consumption Characteristics of Transports Using the Prop-Fan Concept." Boeing Commercial Airplane Co., D6-75780, Oct. 1976; also NASA CR-137937.

5. R. Hirschkron and R. E. Neitzel, "Alternative Concepts for Advanced Energy Conservative Transport Engines." SAE Paper 760536, SAE Air Transportation Meeting, New York, May 1976.

6. R. E. Neitzel, R. Hirschkron, and R. P. Johnston, "Study of Unconventional Aircraft Engines Designed for Low Energy Consumption." General Electric Co., R76AEG597, Dec. 1976; also NASA CR-135136.

7. D. E. Gray and J. W. Witherspoon, "Fuel Conservative Propulsion Concepts for Future Air Transports." SAE Paper 760535, SAE Air Transportation Meeting, New York, May 1976.

8. D. E. Gray, "Study of Unconventional Aircraft Engines Designed for Low Energy Consumption." Pratt & Whitney Aircraft, PWA-5434, June 1976; also NASA CR-135065.

9. J. A. Stern, "Aircraft Propulsion - a Key to Fuel Conservation: An Aircraft Manufacturer's View." SAE Paper 760538, SAE Air Transportation Meeting, New York, May 1976.

10. R. L. Foss and J. P. Hopkins, "Fuel Conservative Potential for the Use of Turboprop Powerplants." SAE Paper 760537, SAE Air Transportation Meeting, New York, May 1976.

11. J. P. Hopkins and H. E. Wharton, "Study of the Cost/Benefit Tradeoffs for Reducing the Energy Consumption of the Commercial Air Transportation System Summary Report." Lockheed-California Co., LR-27769-1, Aug. 1976; also NASA CR-137927.

12. J. P. Hopkins, "Study of the Cost/Benefit Tradeoffs for Reducing the Energy Consumption of the Commercial Air Transportation System Final Report." Lockheed-California Co., LR-27769-2, Aug. 1976; also NASA CR-137926.

13. R. E. Coykendall, et al., "Study of Cost/Benefit Tradeoffs for Reducing the Energy Consumption of the Commercial Air Transportation System." United Air Lines, Inc., June 1976; also NASA CR-137891.

14. F. W. Gobetz and A. A. LeShane, "Cost/Benefit Trade-Offs for Reducing the Energy Consumption of Commercial Air Transportation (RECAT)." United Technologies Research Center, UTRC-R76-912036-17, June 1976; also NASA CR-137878.

15. F. W. Bogetz and A. P. Dubin, "Cost/Benefit Trade-Offs for Reducing the Energy Consumption of Commercial Air Transportation: Final Report." United Technologies Research Center, UTRC-R76-912036-16, June 1976; also NASA CR-138877.

16. D. L. Nored, "Fuel Conservative Aircraft Engine Technology." NASA TM-78962, Sep. 1978.

17. E. F. Kraus, "Cost/Benefit Tradeoffs for Reducing the Energy Consumption of the Commercial Air Transportation System. Vol. 1: Technical Analysis." Douglas Aircraft Co., Inc., MDC-J7340-Vol-1, June 1976; also NASA CR-137923.

J. C. Vanabkoude, "Cost/Benefit Tradeoffs for Reducing the Energy Consumption of the Commercial Air Transportation System. Vol. 2: Market and Economic Analyses." Douglas Aircraft Co., Inc., MDC-J7340-Vol-2, June 1976; also NASA CR-137924.

E. F. Kraus and J. C. Vanabkoude, "Cost/Benefit Tradeoffs for Reducing the Energy Consumption of the Commercial Air Transportation System. Vol. 3: Summary Report." Douglas Aircraft Co., Inc., MDC-J7340, June 1976; also NASA CR-137925.

18. J. P. Hopkins, "Study of the Cost/Benefit Tradeoffs for Reducing the Energy Consumption of the Commercial Air Transportation System. Final Report." Lockheed-California Co., LR-27769-2, Aug. 1976; also NASA CR-137926.

J. P. Hopkins and H. E. Wharton, "Study of the Cost/Benefit Tradeoffs for Reducing the Energy Consumption of the Commerical Air Transportation System. Summary Report." Lockheed-California Co., LR-27769-1, Aug. 1976; also NASA CR-137927.

19. R. L. Foss and J. P. Hopkins, "Fuel Conservative Potential for the Use of Turboprop Powerplants." SAE Paper 760537, SAE Air Transportation Meeting, New York, May 1976.

20. "Energy Consumption Characteristics of Transports Using the Prop-Fan Concept. Final Report." Boeing Commercial Airplane Co., D6-75780, Oct. 1976; also NASA CR-137937. "Energy Consumption Characteristics of Transports Using the Prop-Fan Concept. Summary Report." Boeing Commercial Airplane Co., D6-75780, Nov. 1976. also NASA CR-137938.

21. J. D. Revell and R. H. Tullis, "Fuel Conservation Merits of Advanced Turboprop Transport Aircraft." Lockheed-California Co., LR-28283, Aug. 1977; also NASA CR-152096.

22. D. E. Gray, "Study of Unconventional Aircraft Engines Designed for Low Energy Consumption." Pratt & Whitney Aircraft, PWA-5434, June 1976; also NASA CR-135065.

23. R. E. Neitzel, R. Hirschkron, and R. P. Johnston, "Study of Turbofan Engines Designed for Low Energy Consumption." General Electric Co., R76AEG432, Aug. 1976; NASA CR-135053.

24. R. E. Neitzel, R. Hirschkron, and R. P. Johnston, "Study of Unconventional Aircraft Engines Designed for Low Energy Consumption." General Electric Co.; R76AEG597, Dec. 1976; also NASA CR-135136.

25. D. E. Gray, "Study of Turbofan Engines Designed for Low Energy Consumption." Pratt & Whitney Aircraft, PWA-5318, May 1976; NASA CR-135002.

26. D. E. gray, "Study of Unconventional Aircraft Engines Designed for Low Energy Consumption." Pratt & Whitney Aircraft, PWA-5434, June 1976; NASA CR-135065.

27. R. L. Foss and J. P. Hopkins, "Fuel Conservation Potential for the Use of Turboprop Powerplanes." SAE Paper 760537, SAE Air Transportation Meeting, May 1976.

28. J. P. Hopkins and H. E. Wharton, "Study of the Cost/Benefit Tradeoffs for Reducing the Energy Consumption of the Commercial Air Transportation System. Summary Report." Lockheed-California Co., LR-27769-1, Aug. 1976; also NASA CR-137927.

29. J. P. Hopkins, "Study of the Cost/Benefit Tradeoffs for Reducing the Energy Consumption of the Commercial Air Transportation System. Final Report." Lockheed-California Co., LR-27769-2, Aug. 1976; also NASA CR-137926.

30. J. Stern, "Aircraft Propulsion - A Key to Fuel Conservation: An Aircraft Manufacturer's View." SAE Paper 760538, SAE Air Transportation Meeting, New York, May 1976.

31. E. F. Kraus, "Cost/Benefit Tradeoffs for Reducing the Energy Consumption of Commercial Air Transportation System. Vol. I: Technical Analysis." Douglas Aircraft Co., Inc., MDC-J7340-Vol.-1, June 1976; also NASA CR-137923.

32. J. C. Vanabkoude, "Cost/Benefit Tradeoffs for Reducing the Energy Consumption of Commercial Air Transportation System. Vol. II: Market and Economic Analysis." Douglas Aircraft Co., Inc., MDC-J7340-Vol.-2, June 1976; also NASA CR-137924.

33. "Energy Consumption Characteristics of Transports Using the Prop-Fan Concept. Summary Report." Boeing Commercial Airplane Co., D6-75780, Nov. 1976; also NASA CR-137938.

34. "Energy Consumption Characteristics of Transports Using the Prop-Fan Concept. Final Report." Boeing Commercial Airplane Co., D6-75780, Oct. 1976; also NASA CR-137937.

35. C. Rohrbach, "A Report on the Aerodynamic Design and Wind Tunnel Test of a Prop-Fan Model." AIAA Paper No. 76-667, AIAA/SAE 12th Propulsion Conference, Palo Alto. July 1976.

36. C. Rohrbach and F. B. Metzger, "The Prop-Fan - A New Look in Propulsors." AIAA Paper 75-1208, AIAA/SAE 11th Propulsion Conference, Anaheim, Sep. 1975.

37. C. Rohrbach, "A Report on the Aerodynamic Design and Wind Tunnel Test of a Prop-Fan Model." AIAA Paper 76-667, AIAA/SAE 12th Propulsion Conference, Palo Alto, July 1976.

38. D. B. Hanson, "Near Field Noise of High Tip Speed Propellers in Forward Flight." AIAA Paper 76-565, AIAA 3rd Aero-Acoustics Conference, Palo Alto, July 1976.

39. F. B. Metzger and C. Rohrbach, "Aeroacoustic Design of the Prop-Fan." AIAA 79-0610, AIAA 5th Aero-Acoustics Conference, Seattle, Mar. 1979.

40. R. J. Swallow and R. A. Aiello, "NASA Lewis 8- by 6-Foot Supersonic Wind Tunnel." NASA TM X-71542, May 1974.

41. R. M. Reynolds, R. I. Sammonds, and G. C. Kenyon, "An Investigation of a Four-Blade Single-Rotation Propeller in Combination With an NACA 1-Series D-Type Cowling at Mach Numbers Up to 0.83." NACA RMA53B06, Apr. 1953.

42. H. Glauert, "Airplane Propellers, Div. L, Chapt. VIII, Body and Wing Interference." Aerodynamic Theory, Vol. IV, W. F. Durand, editor, Berlin: Julius Springer, 1935.

43. D. M. Black, R. W. Menthe, and H. S. Wainauski, "Aerodynamic Design and Performance Testing of an Advanced 30° Swept, Eight Bladed Propeller at Mach numbers from 0.2 to 0.85." NASA CR-3047, Sep. 1978.

44. J. H. Dittmar, B. J. Blaha, and R. J. Jeracki, "Tone Noise of Three Supersonic Helical Tip Speed Propellers in a Wind Tunnel at 0.8 Mach number." NASA TM-79046, Dec. 1978.

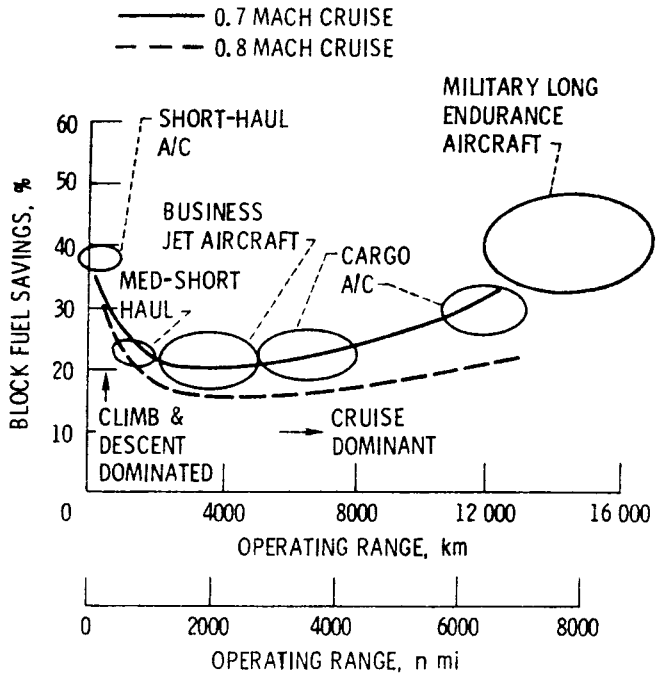

Figure 1. - Fuel saving trends of advanced turboprop (prop-fan) powered aircraft over comparable turbofan powered aircraft.

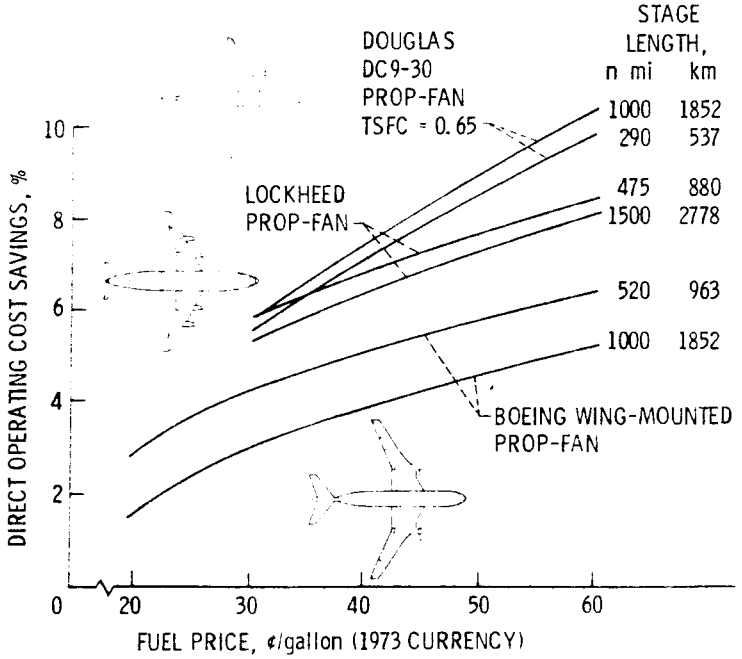

Figure 2. - Advanced turboprop (prop-fan) aircraft operating cost savings.

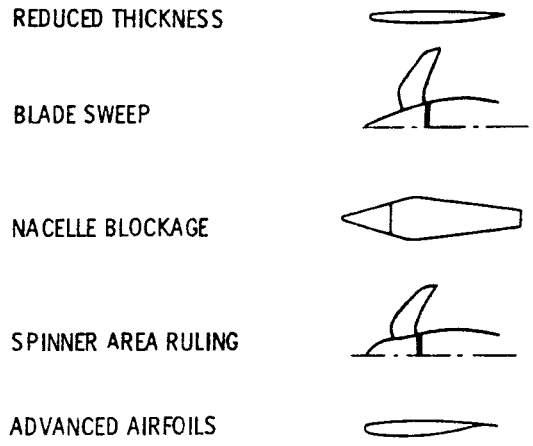

Figure 3. - Advanced aerodynamic concepts for improving propeller performance.

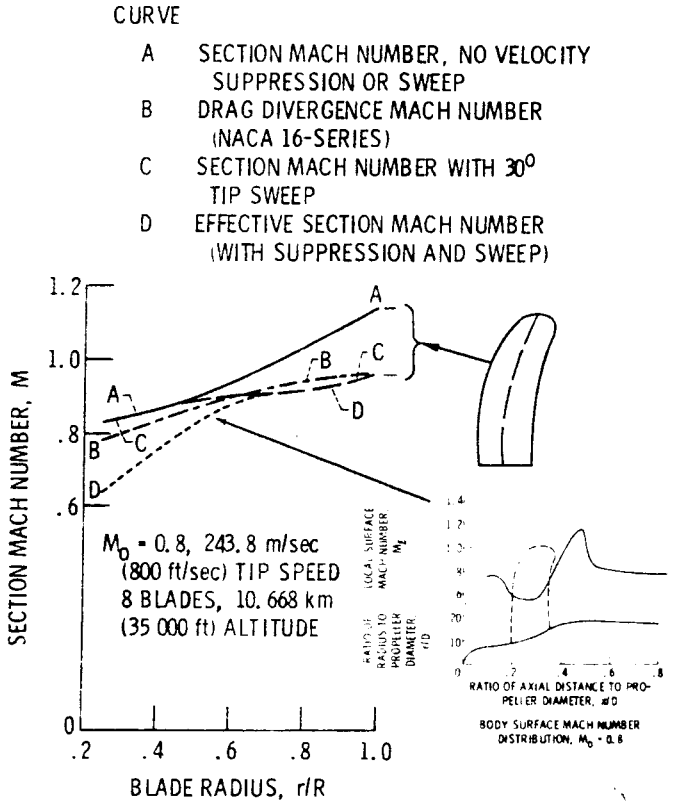

Figure 4. - Effects of advanced aerodynamic concepts on blade section Mach number distributions.

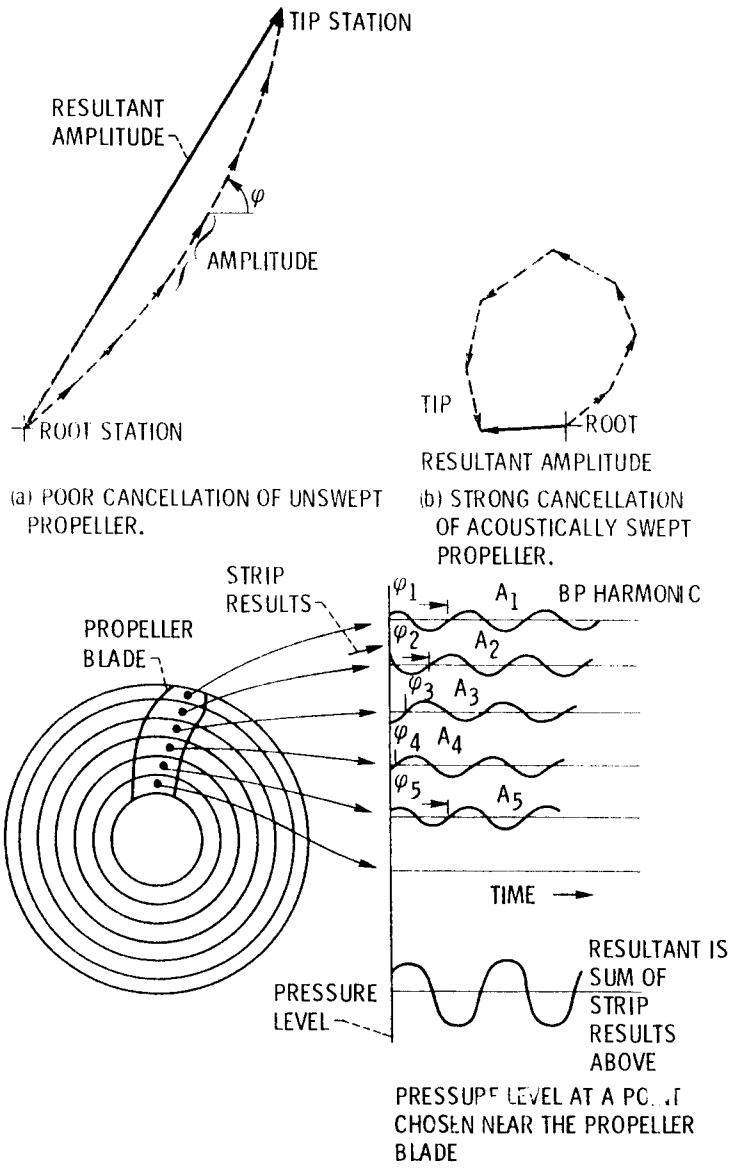

Figure 5. - Acoustic strip analysis technique for near-field noise reduction.

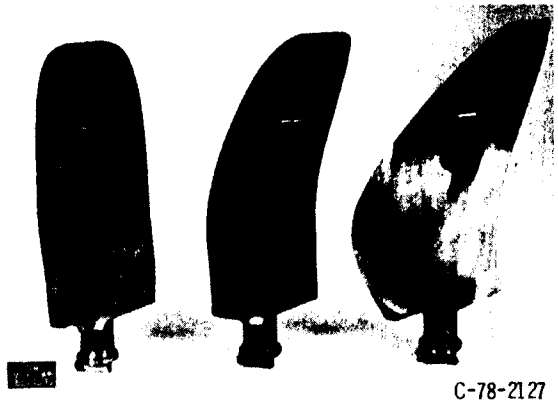

C-78-2127

	SR-2	SR-1, 1M	SR-3
TIP SPEED, m/sec (ft/sec)	244 (800)	244 (800)	244 (800)
POWER LOADING, P/D^2, kW/m^2 (shp/ft^2)	301 (37.5)	301 (37.5)	301 (37.5)
NO. OF BLADES	8	8	8
TIP SWEEP ANGLE, deg	0	30	45
DESIGN EFF., %	76.6	78.9, 79.3	81
DESIGN NOISE LEVEL, dB	143	143	137

Figure 6. - Design characteristics and planform of high-speed propeller models.

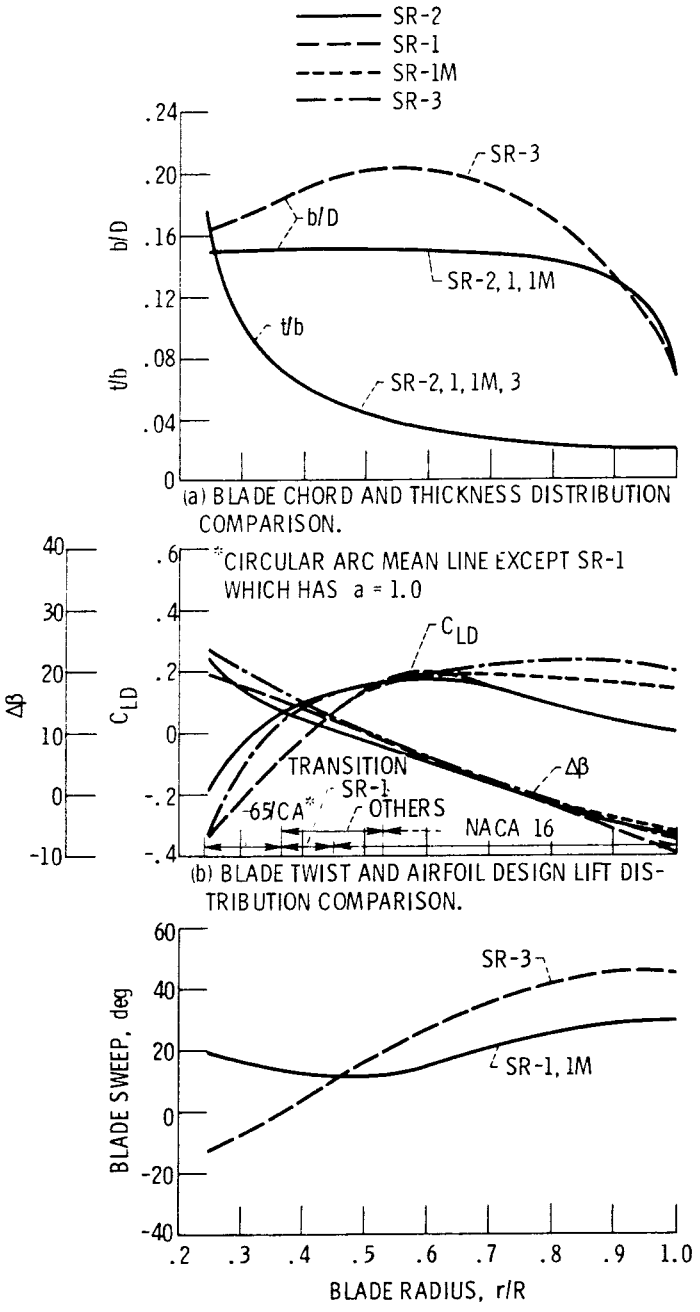

Figure 7. - Blade geometry characteristics.

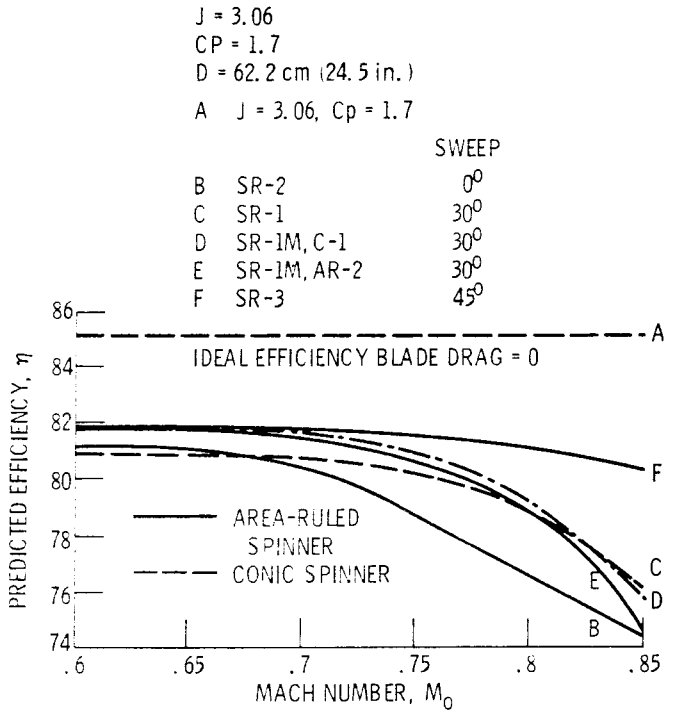

Figure 8. - Predicted performance of 8 bladed propellers.

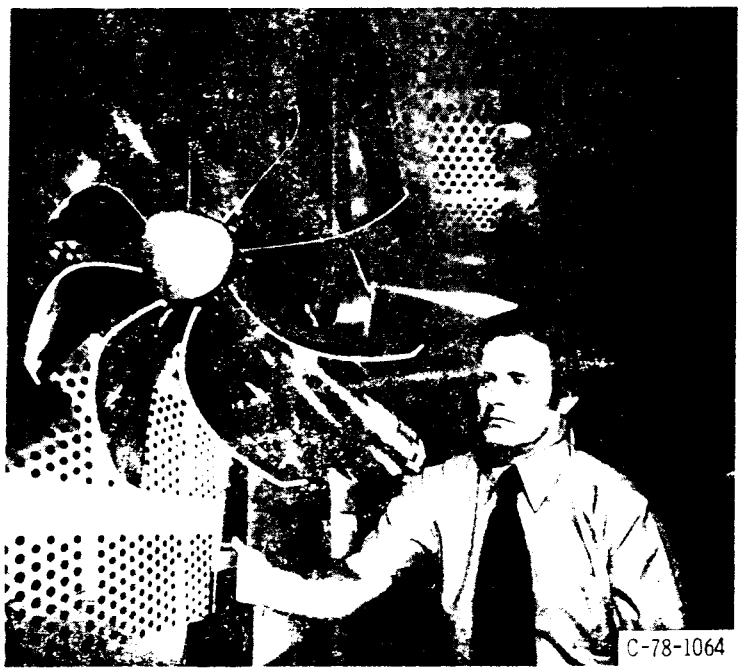

Figure 9. - Installation of SR-3 propeller model in the Lewis 8-by-6 foot wind tunnel.

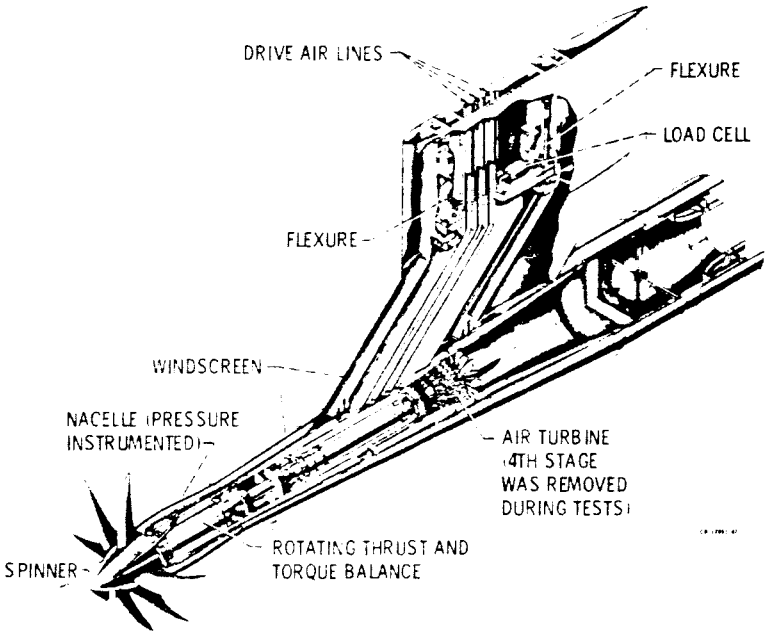

Figure 10. - Cutaway view of strut-mounted Lewis propeller test rig.

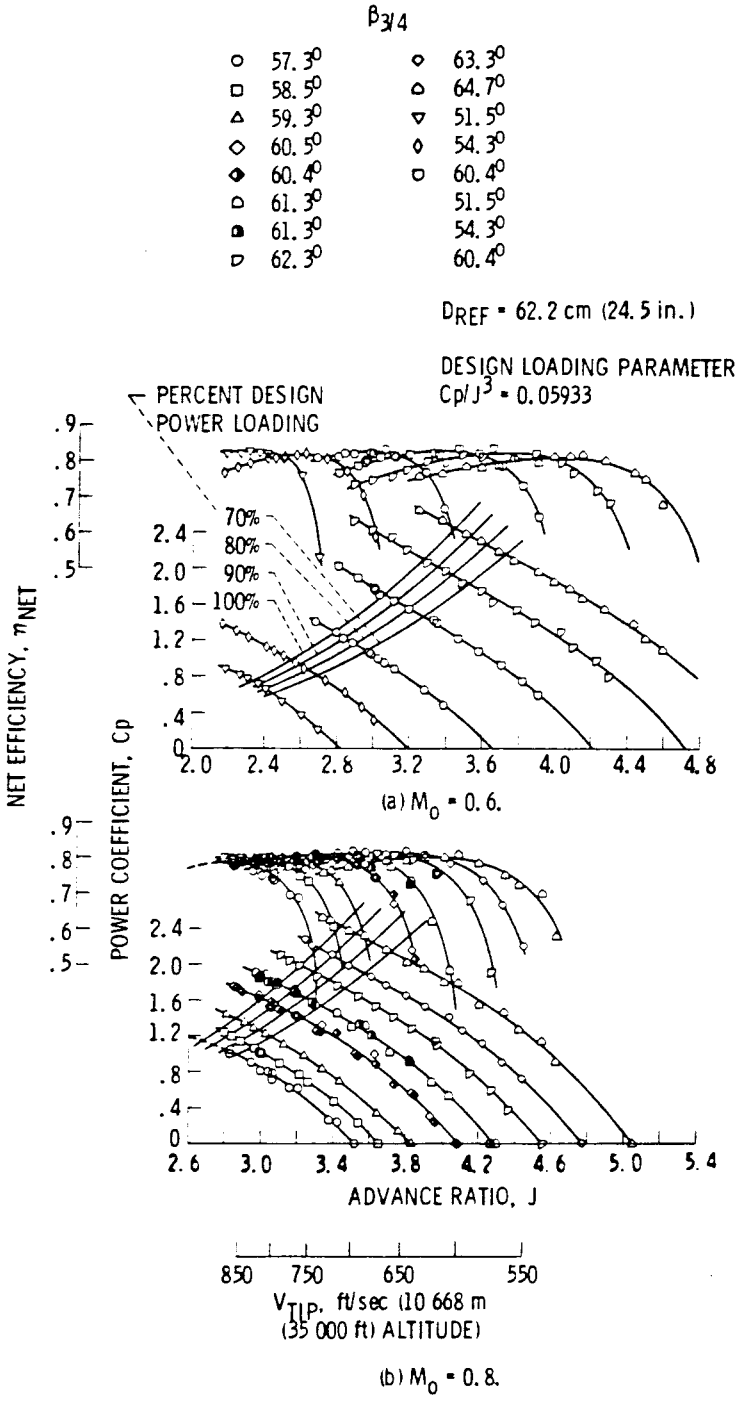

Figure 11. - Basic measured performance for SR-3, 45° swept propeller.

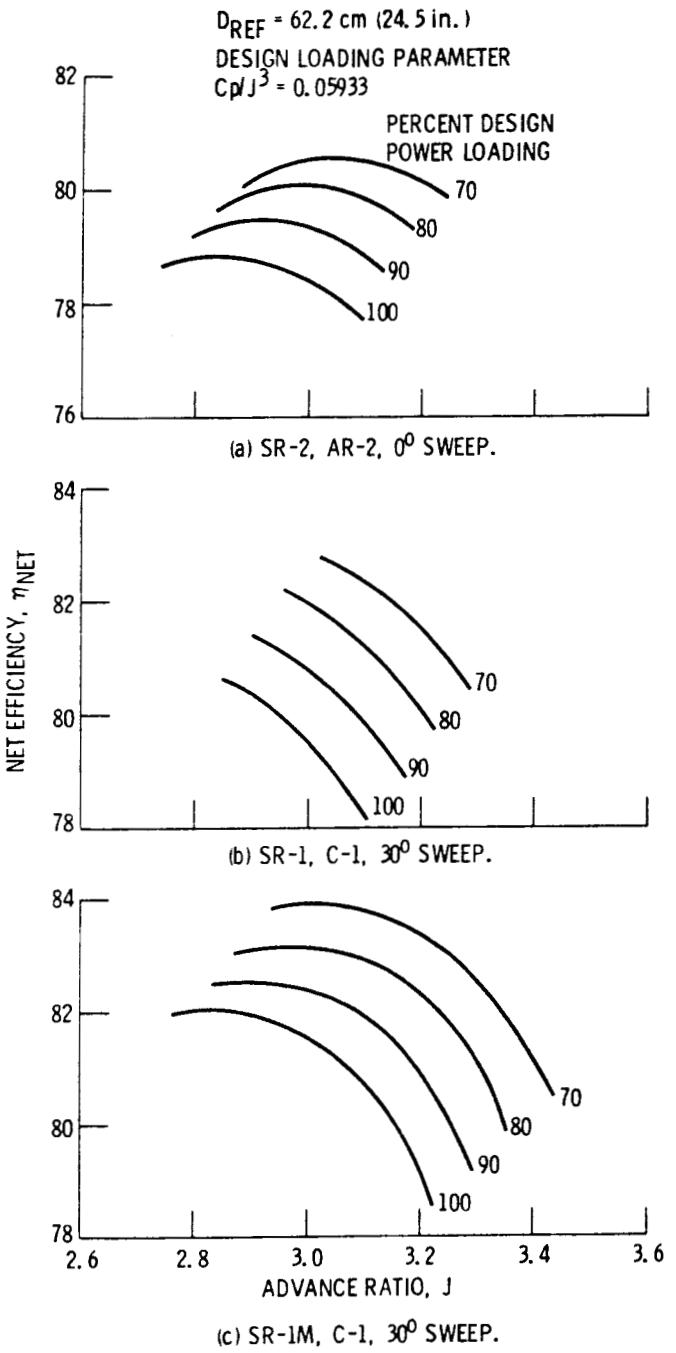

Figure 12. - Effect of power loading and advance ratio on net efficiency at Mach 0.6.

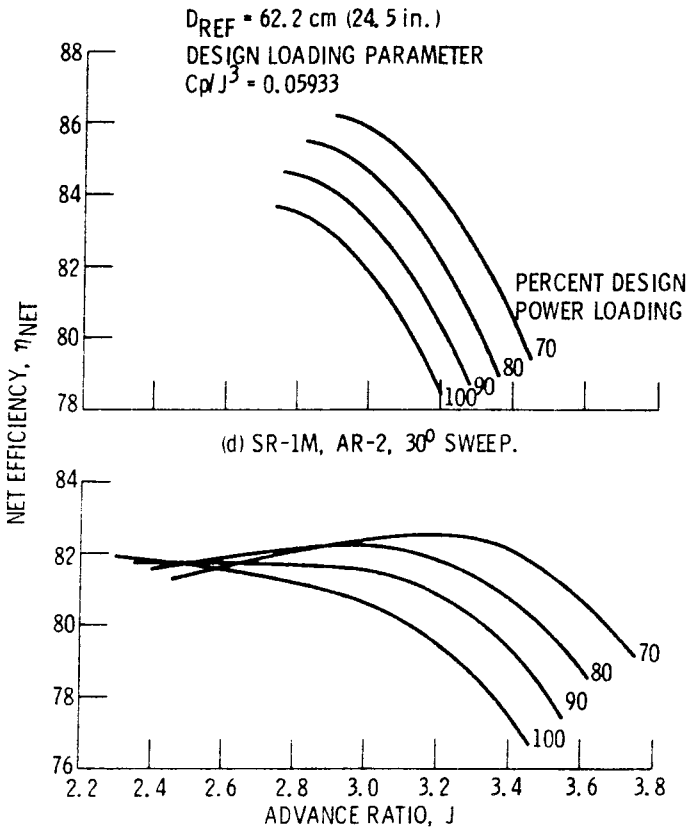

(d) SR-1M, AR-2, 30° SWEEP.

(e) SR-3, AR-3, 45° SWEEP.

Figure 12. - Concluded.

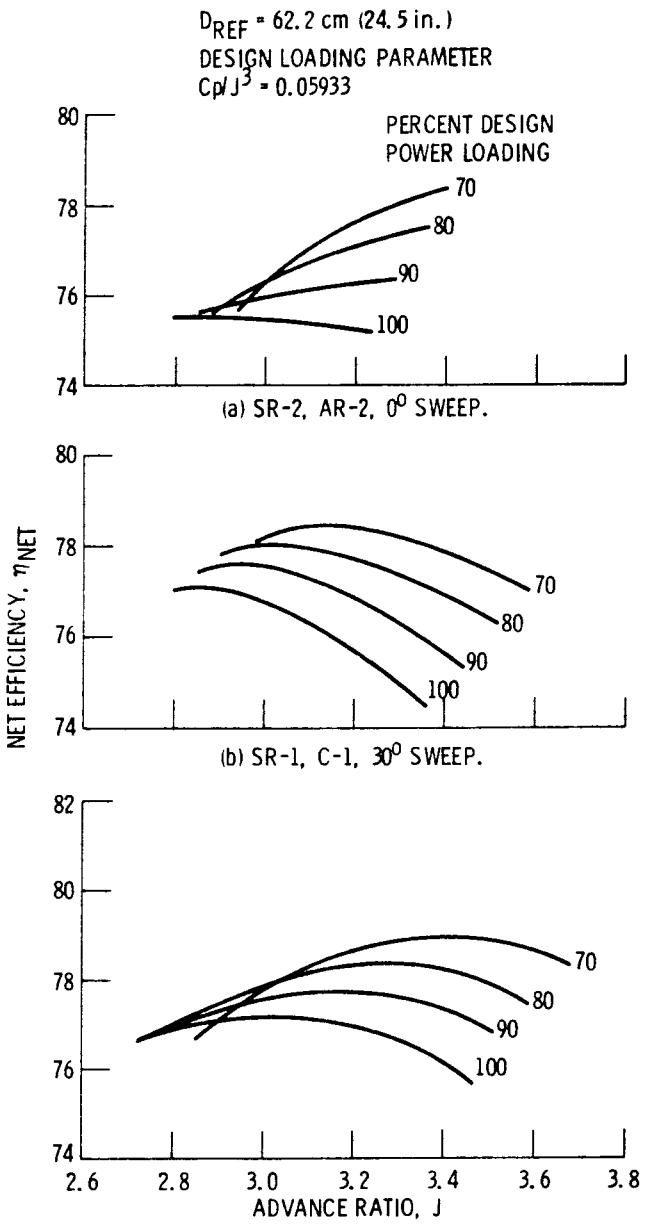

Figure 13. - Effect of power loading and advance ratio on net efficiency at Mach 0.8.

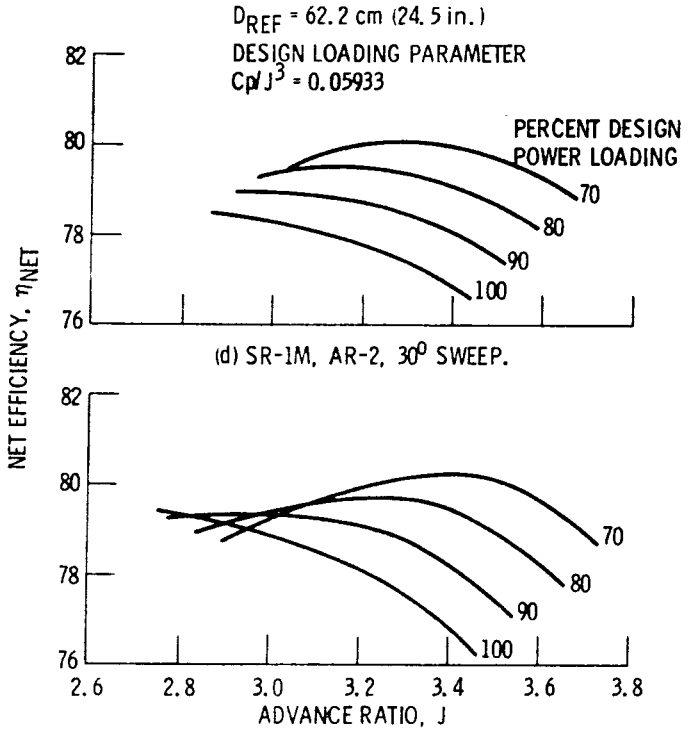

(d) SR-1M, AR-2, 30° SWEEP.

(e) SR-3, AR-3, 45° SWEEP.

Figure 13. - Concluded.

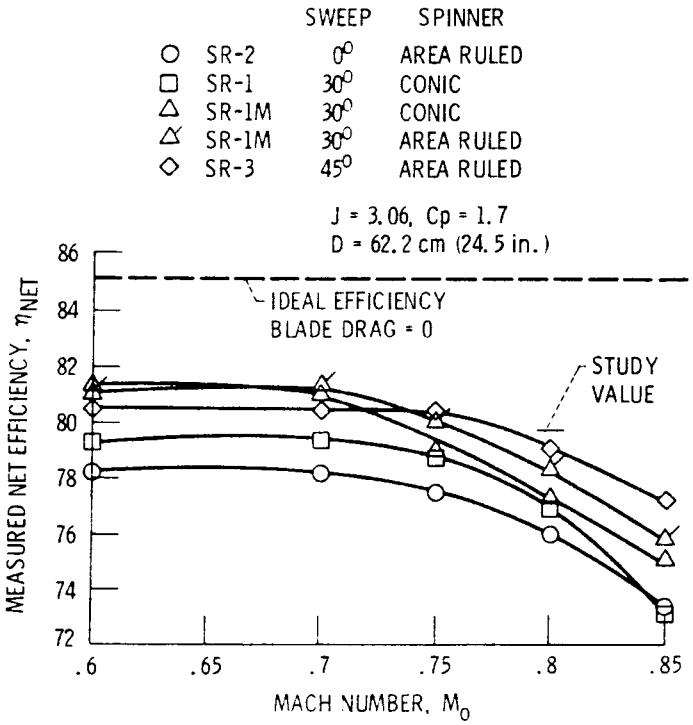

Figure 14. - High speed propeller performance summary.

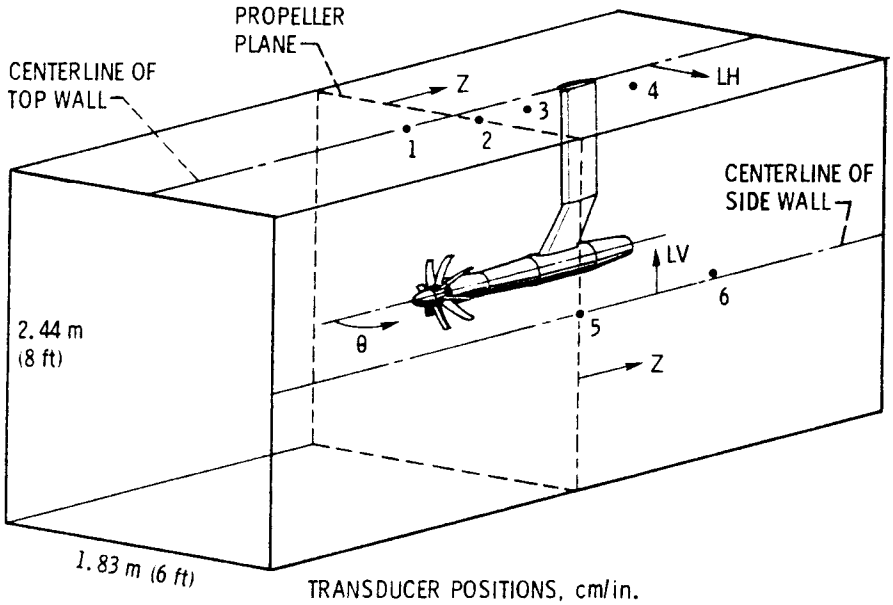

TRANSDUCER POSITIONS, cm/in.

POSITIONS	1	2	3	4	5	6
Z	-27.7 -10.9	0.953 0.375	45.2 17.8	104.4 41.1	-0.15 -0.06	105.4 41.5
LH	2.54 1.0	10.2 4.0	7.62 3.0	31.5 12.4	91.4 36.0	91.4 36.0
LV	121.9 48.0	121.9 48.0	121.9 48.0	121.9 48.0	6.35 2.5	1.78 0.7
NOMINAL ANGLE, θ	77^{0}	90^{0}	110^{0}	130^{0}	90^{0}	139^{0}

Figure 15. - Pressure transducer positions.

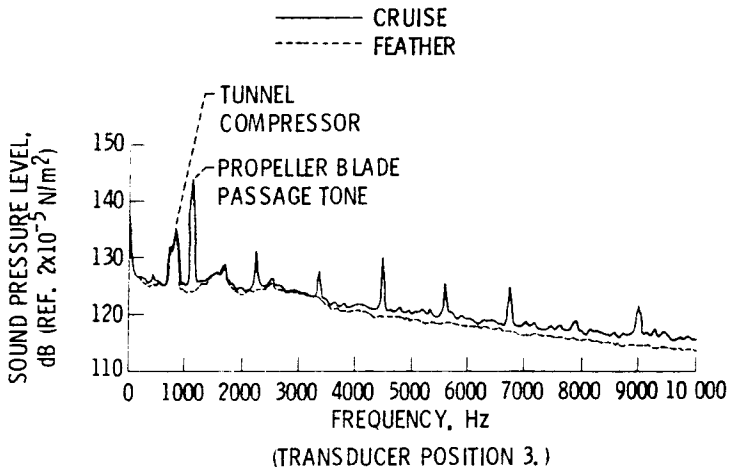

Figure 16. - Typical comparison of SR-3 propeller at cruise and feather.

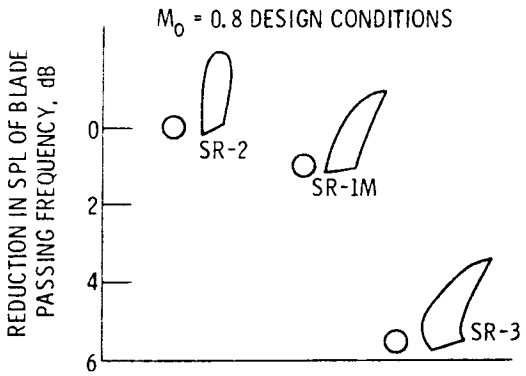

Figure 17. - Measured noise comparison of propeller models.

1 Report No. NASA TM-79124	2 Government Accession No.	3. Recipient's Catalog No.
4 Title and Subtitle WIND TUNNEL PERFORMANCE OF FOUR ENERGY EFFICIENT PROPELLERS DESIGNED FOR MACH 0.8 CRUISE		5. Report Date 6. Performing Organization Code
7 Author(s) Robert J. Jeracki, Daniel C. Mikkelson, and Bernard J. Blaha		8. Performing Organization Report No. E-9960 10. Work Unit No.
9 Performing Organization Name and Address National Aeronautics and Space Administration Lewis Research Center Cleveland, Ohio 44135		11. Contract or Grant No. 13. Type of Report and Period Covered Technical Memorandum
12 Sponsoring Agency Name and Address National Aeronautics and Space Administration Washington, D.C. 20546		14. Sponsoring Agency Code

15 Supplementary Notes

16 Abstract

The increased emphasis on fuel conservation has stimulated a renewed interest in turboprop powered aircraft. Recent studies by NASA and industry indicate that fuel savings from 15 to 30 percent at Mach 0.8 may be realized by the use of an advanced high-speed turboprop, and over 20% at Mach 0.7 typical of business jet aircraft. This aircraft must be capable of high efficiency at Mach 0.8 cruise above 9.144 km (30 000 ft) altitude if it is to compete with turbofan powered aircraft. In the past, propellers were highly efficient at cruise speeds up to approximately Mach 0.6. However, above this speed, large compressibility losses on the propeller blading caused the efficiency to fall rapidly. If these losses are to be overcome, new design concepts will have to be developed for advanced high-speed propellers. Several advanced aerodynamic and acoustic concepts were investigated in recent wind tunnel tests performed in the NASA-Lewis Research Center 8x6 foot wind tunnel. These concepts included aerodynamically integrated propeller/nacelles, area-ruling, blade sweep, reduced blade thickness, and power (disk) loadings several times higher than conventional designs. Four eight-bladed propeller models were tested to determine aerodynamic performance. Relative noise measurements were made on three of the models at cruise conditions. Three of the models were designed with swept blades and one with straight blades. At the design Mach number of 0.8, power coefficient of 1.7, and advance ratio of 3.06, the straight bladed model had the lowest net efficiency of 75.8%. Increasing the sweep to 30° improved the performance to near 77%. Installation of an area-ruled spinner on a 30° sweep model further improved the efficiency to about 78%. The model with the highest blade sweep (45°) and an area-ruled spinner had the highest net efficiency of 78.7%, and at lower power loadings the efficiency exceeded 80%. At lower Mach numbers the 30° swept model had the highest efficiency. Values near 81% were obtained for the design loading at speeds to Mach 0.7. Relative noise measurements indicated that the acoustically designed 45° sweep model reduced the near field cruise noise by between 5 and 6 dB.

17 Key Words (Suggested by Author(s))	18 Distribution Statement
Fuel conservation Advanced turboprop Propeller Noise reduction	Unclassified - unlimited STAR Category 02

19. Security Classif. (of this report)	20. Security Classif. (of this page)	21. No. of Pages	22. Price*
Unclassified	Unclassified		

* For sale by the National Technical Information Service, Springfield, Virginia 22161